

# IMPACT OF FROND MOISTURE CONTENT ON CUTTING FORCES IN OIL PALM HARVESTING

UMESH GANESH<sup>1</sup>; ZAIDI MOHD RIPIN<sup>1</sup>; WAN MOHD AMRI WAN MAMAT ALI<sup>1</sup>;  
AMIRUL AMZAR JA'FAR<sup>1</sup> and MOHAMAD IKHWAN ZAINI RIDZWAN<sup>1\*</sup>

## ABSTRACT

Oil palm frond (OPF) is a major agricultural by-product whose mechanical behaviour controls harvesting operations. This study investigates how moisture content (MC) affects the cutting force and mechanical behaviour of OPF when using a cordless electric reciprocating saw. Optimising the handling of OPF, a major oil palm by-product, is important for improving sustainability and harvesting efficiency. OPF samples were classified into four moisture categories: Fresh (75%–100%), moderately dry (50%–75%), dry (25%–50%), and very dry (0%–25%). Cutting force was measured using a load cell, while mechanical properties were assessed through three-point bending tests and porosity was determined via scanning electron microscopy. Results show that the cutting force and specific cutting force (SCF) decrease significantly as MC increases. The driest samples required the highest cutting effort, while fresher ones were easier to cut. Flexural strength and stiffness increased as moisture decreased, while porosity declined. These findings highlight the importance of moisture in tool performance and support the development of more ergonomic, energy-efficient and automated harvesting solutions.

**Keywords:** cutting force, mechanical properties, moisture content, oil palm frond (OPF) sustainability.

**Received:** 20 October 2024; **Accepted:** 5 November 2025; **Published online:** 26 January 2026.

## INTRODUCTION

Oil palm plantations are a vital component of tropical agriculture, providing a major source of palm oil used in numerous products worldwide, from food and cosmetics to biofuels (Ganesh et al., 2024; Noor & Ridzwan, 2024). An oil palm tree (*Elaeis guineensis*) is valued not only for its fruit but also for its fronds, which are typically regarded as a by-product. Oil palm frond (OPF), often considered an underutilised part of the oil palm tree and is typically left to decompose between rows of palm trees. This practice supports soil conservation, erosion control, and long-term nutrient recycling. Given the large quantities of fronds produced annually by plantations, OPF represents a promising resource.

These fronds can be used in various applications, including as fibre feed for ruminants (Hamdan et al., 2012), as well as for composting and biomass energy production (Guangul et al., 2013). Efficient harvesting of OPF is fundamental for improving the use of these by-products and ensuring the economic sustainability of the plantation (Ganesh et al., 2025). OPF also have potential applications in product manufacturing. OPF can be used in the production of biodegradable products, renewable sources for carbon and ethanol production, and as raw materials in the pulp and paper industry (Ooi et al., 2017) or generating bioenergy (Saminathan et al., 2022).

Moisture content (MC) is a critical factor in agriculture that influences the physical properties of various crops and by-products (Moya-Ignacio et al., 2024). In different agricultural contexts, such as cereal and grain harvesting, MC affects cutting and processing efficiency. Similarly, in forestry, moisture levels impact the ease of timber processing. In food processing, MC affects the cutting and slicing of vegetables, fruits and meat products.

<sup>1</sup> Neurorehabilitation Engineering and Assistance Systems Research, School of Mechanical Engineering, Engineering Campus, Universiti Sains Malaysia, 14300 Nibong Tebal, Penang, Malaysia.

\* Corresponding author e-mail: [mikhwanz@usm.my](mailto:mikhwanz@usm.my)

Understanding how MC affects these processes can lead to more efficient and effective harvesting and processing techniques (Beljo-Lucic et al., 2004). Efficient harvesting and processing of these fronds are crucial for maximising their utility and minimising waste. Despite well-documented effects of moisture on different agricultural materials, there is limited study focused specifically on how MC can affect the cutting forces and mechanical properties of OPF.

To fully consume the OPF in various real-world applications, this study addresses a critical research gap by investigating the impact of MC on OPF. Recent advancements in oil palm harvesting tools (Ahmad, 2024; Chan et al., 2022; Ganesh et al., 2024) focused on motorisation and ergonomics, but the interaction between frond material and tool performance or required cutting force remains underexplored. This study contributes novel insight into how frond moisture levels influence cutting resistance, an area not previously quantified in the context of oil palm harvesting, thereby supporting the design of energy-efficient and ergonomically improved tools. The objective is to determine how MC affects cutting force during OPF cutting using an electric reciprocating saw. It also examines how MC influences the strength of the fronds, measured by flexural load and their porosity.

## MATERIALS AND METHODS

### Fronds Preparation

A total of 20 OPF were prepared, with five fronds assigned to each MC level. All samples were taken from the basal portion (40 cm in length) of 10–15 years old oil palm trees to ensure consistency in width and thickness. For Level 1 (fresh fronds), no drying was performed. For Level 2, 3 and 4, the fronds were dried in the oven at 70°C to reduce their MC. Prior to drying, the initial weight of each frond was recorded using a digital weighing scale. The drying durations were set at 24 hr for Level 2, 48 hr for Level 3 and 71 hr for Level 4. After the drying process, the final weight was measured and the MC was calculated using Equation (1), following the method reported by Sulaiman et al. (2016) and Ozigi et al. (2018).

$$\text{Moisture content (\%)} = \frac{w-d}{w} \times 100 \quad (1)$$

where,  $w$  and  $d$  represent the wet weight and weight after drying, respectively.

Each frond was used sequentially for all three experimental procedures; cutting force

measurement, bending strength test and porosity analysis via scanning electron microscopy (SEM). These procedures ensured that all tests were performed on the same material, allowing direct correlation between mechanical and microstructural properties. All experiments were conducted immediately after the frond preparation.

### Experimental Procedures

In this study, a cordless electric reciprocating saw (WORX WG894E, Positec Tool Corp, Suzhou, China) was used to investigate the cutting forces required to cut the OPF samples. The saw outputs approximately 45–55 Watts (25V–28V, 1.3A–1.6A) and operates at 2,200 rpm. A cutting machine clamp equipped with a height-adjustable jack and a ball screw actuator system (HANPOSE 23HS10028 260N·cm, Guangzhou, China) was used to convert rotational motion into precise linear motion, allowing for an automatic feed rate of 5 mm/s. All tests were performed in a controlled indoor environment with ambient temperature between 24°C–25°C and relative humidity of 60%–63%. The entire system ensured stable and repeatable cutting conditions throughout the experiments.

**Experiment setup.** To achieve high repeatability in the setup, the frond was consistently clamped perpendicular to the saw blade using a fixed-position jig (Figure 1a). A 3-axis load cell (MLD66, Michigan Scientific Corp., USA) with a capacity of 300 N and an 80 Hz sampling rate was employed to measure the cutting forces. The load cell was calibrated using known masses of a 10–30 N weight plate. Alignment between the cutting direction and the load cell axis was maintained (Figure 1b), and the load cell was rigidly mounted between the electric saw and the actuator base to eliminate variation from machine vibration or misalignment (Figure 1c). These measures ensured experimental repeatability across all samples and moisture levels.

For the frond samples with MCs in Level 1, the experiment was conducted using five fronds. The load cell readings were recorded during the experiment. After each frond was cut, the cut end was taken, placed on a clear white background and photographed using a high-resolution camera. The image was then analysed using ImageJ software to determine the cross-sectional area, which was used to normalise the recorded cutting force. After cutting the fronds, two additional steps were performed. The first was preparing samples for porosity measurement SEM, and the second was measuring the strength (bending test).

**SEM analysis.** For SEM analysis, a Hitachi S-3400N variable-pressure SEM (Hitachi High-Tech, Tokyo, Japan) was used (Figure 2a). The samples were cut

into  $10 \times 10 \times 10$  mm pieces (Figure 2b), following BS 373 standards (Ratanawilai et al., 2006). The SEM analysis worked under a vacuum pressure method to capture the porosity of the fronds, with electron imaging conducted at an acceleration voltage of 15 kV (Abdullah et al., 2012).

**Bending test.** The bending test was conducted using a 3-point setup on an Instron machine (Instron 3367, USA) (Figure 3a), applying load until the frond's elongation exceeded its structural limits, causing the cell structure to break. The samples were prepared at the dimensions of  $300 \times 20 \times 20$  mm (Figure 3b), and the results were obtained through the synchronised software, Bluehill 2 (version 2.26, Instron, USA).

For the remaining moisture levels, the experiment was conducted following the desired drying oven time. The same methods were used to measure the cutting force, SEM analysis and bending test across all MC levels. To ensure consistent cutting performance throughout the study, the saw blade was inspected and cleaned after every cut. Blade wear was minimal, and no replacement was necessary during the experiments.

## Data Processing

The recorded cutting force data was then processed using Python to filter out noisy data and

obtain smooth, accurate measurements. The raw data were smoothed by applying a Savitzky-Golay filter with a window size of 10 and a polynomial order of three, which helps in preserving the high-frequency components while reducing noise in the signal. The resultant cutting force was calculated using Python, according to the following Equation (2).

$$F_{\text{resultant}} = \sqrt{F_x^2 + F_y^2 + F_z^2} \quad (2)$$

where,  $F_x$ ,  $F_y$  and  $F_z$  represent the forces measured along the x, y and z axes, respectively. The cutting force was normalised with respect to the frond cross-sectional area to determine the Specific Cutting Force (SCF) as shown in Equation (3).

$$\text{SCF} = \frac{F_{\text{peak resultant}}}{A} \quad (3)$$

where,  $F_{\text{peak resultant}}$  is obtained from Equation (1),  $A$  represent the cross-sectional area of the frond.

## Statistical Analysis

The collected cutting force data were analysed using descriptive statistical methods, including mean and standard deviation (SD). To understand the relationships and dependencies among the

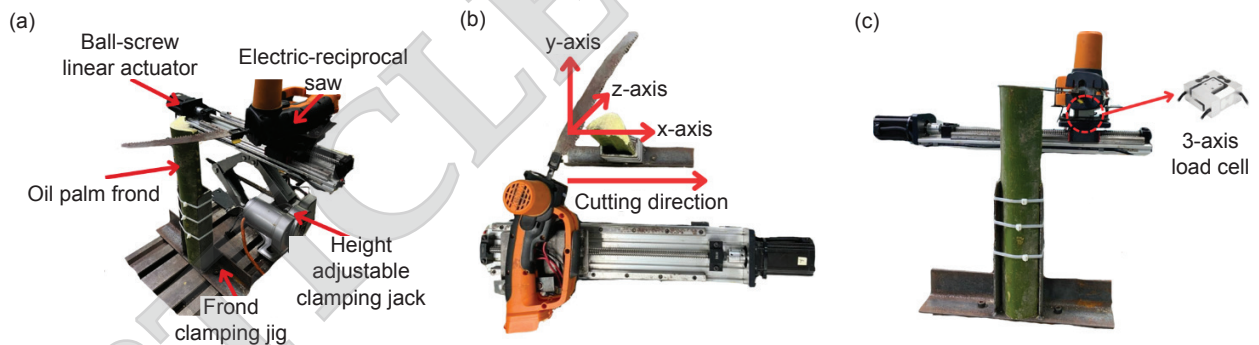


Figure 1. (a) Experiment setup, (b) load cell axis and cutting direction and (c) load cell location.

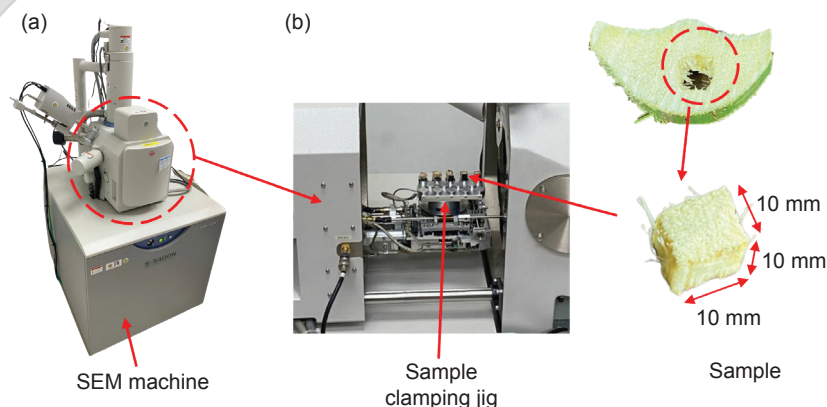


Figure 2. (a) SEM machine and (b) sample for SEM analysis.

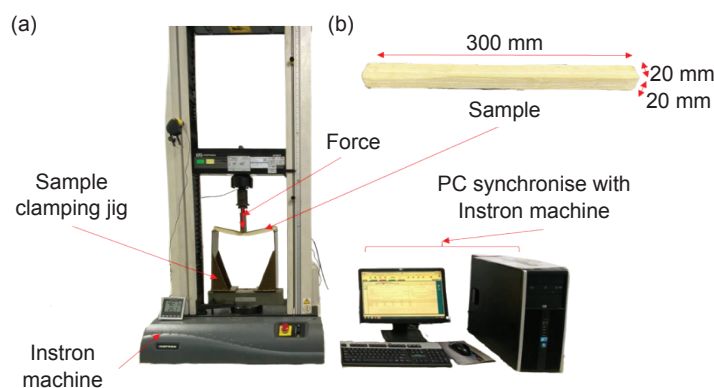


Figure 3. (a) Instron machine, and (b) sample for bending test.

variables, Pearson’s correlation coefficients were calculated between the cutting force, MC, flexural load, Young’s modulus and porosity, using IBM SPSS Statistical software.

Additionally, a t-test was conducted to compare the cutting forces across different moisture levels, aiming to determine the significance of the differences in cutting forces due to variations in MC.

## RESULTS AND DISCUSSION

The MC and corresponding weight data of the fronds are presented in Table 1. The load cell data were recorded along the x, y and z axes (Figure 4a), and the resultant cutting force was calculated. The resultant force was then smoothed using a Savitzky-Golay filter to reduce noise and preserve critical signal details (Figure 4b). For the bending test, the flexural load and flexure

extension were measured and obtained graphs using the Instron machine’s synchronised software (Figure 5a). For the porosity analysis, images were captured at a magnification scale of 300x (100 μm). The porosity of each frond sample was subsequently calculated using ImageJ software (version: 1.54 g), where the images were processed by splitting channels, applying a threshold set at 0–50 to highlight the dark porosity spots and analysing particle areas to calculate the porosity percentage.

The cutting force required for OPF harvesting varied significantly with the MC of the fronds (Figure 6). For the driest fronds (0%–25% moisture), the mean cutting force is the highest at  $53.00 \pm 2.62$  N. As MC increased to the 25%–50% range, the cutting force decreased to a mean value of  $44.77 \pm 4.37$  N. When the MC is further increased into the 50%–75% range, the mean cutting force has decreased to  $25.92 \pm 2.18$  N. The highest

TABLE 1. OIL PALM FROND MOISTURE CONTENT

Moisture level	Moisture range (%)	Frond sample	Initial weight (g)	Final weight (g)	Oven-dry temperature (°C)	Oven-dry duration (hr)	Calculated moisture (%)	Avg. calculated moisture (%)
1	75–100 (fresh)	1	503.31					Fresh
		2	558.99					
		3	521.77	-	-	-	-	
		4	513.39					
		5	539.09					
2	50–75	6	417.37	298.28			60.07	$65.64 \pm 6.00$
		7	466.74	374.18			75.26	
		8	461.89	334.58	70	24	61.95	
		9	486.85	356.93			63.60	
		10	498.80	375.96			67.33	
3	25–50	11	483.08	305.36			41.80	$38.36 \pm 9.46$
		12	462.38	312.21			51.90	
		13	432.60	267.51	70	48	38.29	
		14	558.99	322.61			26.73	
		15	503.87	301.89			33.09	
4	0–25 (driest)	16	588.78	305.35			7.18	$10.72 \pm 4.50$
		17	533.36	289.78			15.94	
		18	703.27	370.88	70	71	10.38	
		19	564.40	290.28			5.57	
		20	547.41	295.17			14.55	

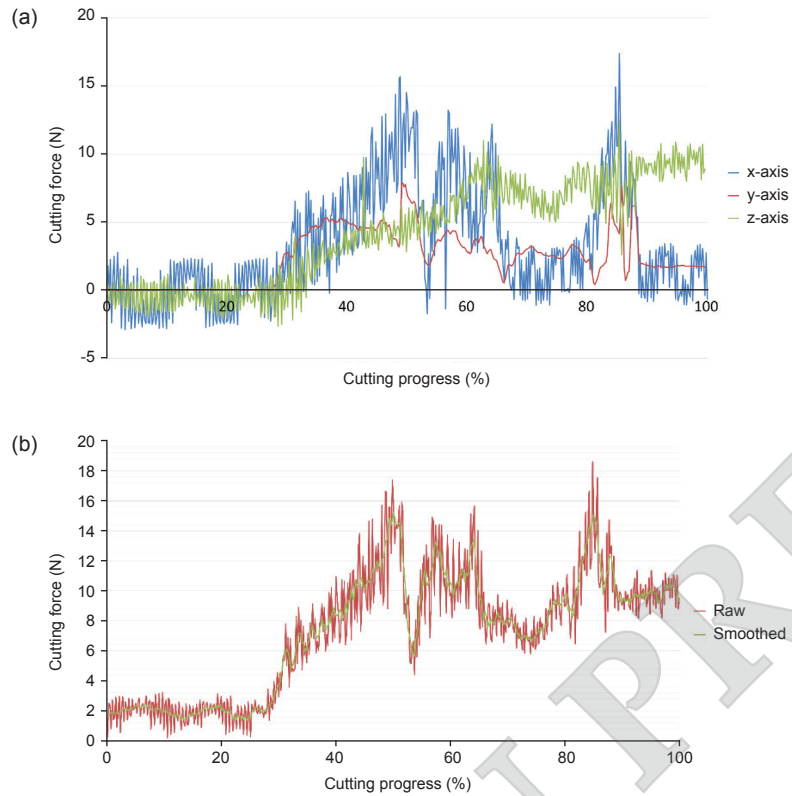


Figure 4. (a) Raw load cell data for x, y and z axis and (b) Raw and smoothed resultant cutting force data.

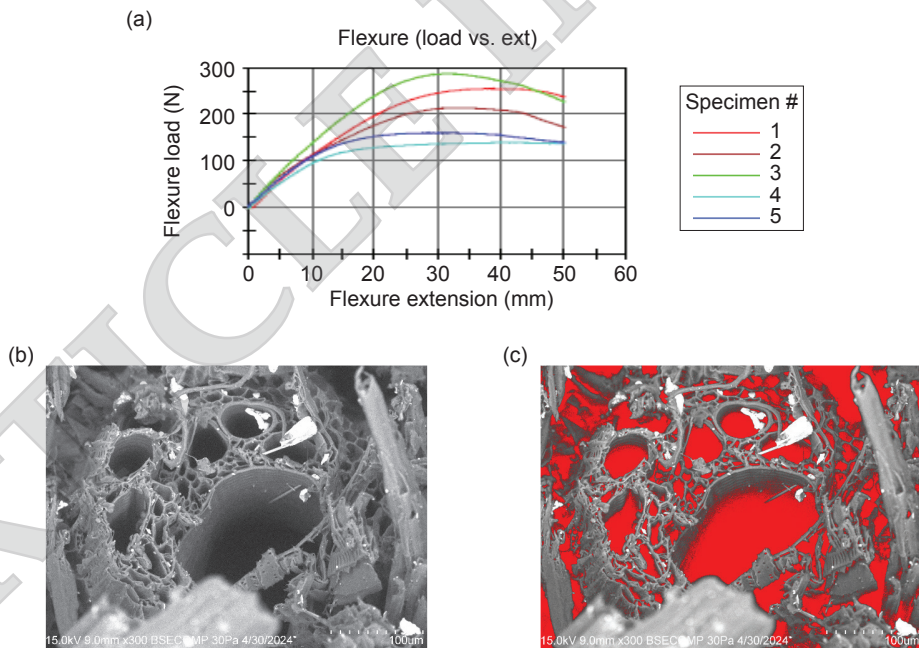


Figure 5. (a) Bending test result, (b) porosity captured using SEM, and (c) porosity area calculation.

moisture level (75%–100%) required the least cutting force, with a mean of  $14.07 \pm 0.68$  N. These results demonstrate that drier fronds require more force to cut, likely due to their increased stiffness. Pairwise independent t-tests confirmed significant differences between 0%–25% and 75%–100% ( $p = 0.016$ ), and between 25%–50% and 75%–100% ( $p = 0.028$ ), as indicated by asterisks in Figure 6.

The cutting force required to harvest OPF decreases significantly with increasing MC. The driest fronds (0%–25% moisture) required the highest mean cutting force of  $55.0 \pm 4.0$  N, while the most saturated fronds (75%–100% moisture) required only  $25.0 \pm 2.5$  N. This inverse relationship between cutting force and MC is due to the increased rigidity and stiffness of drier fronds,

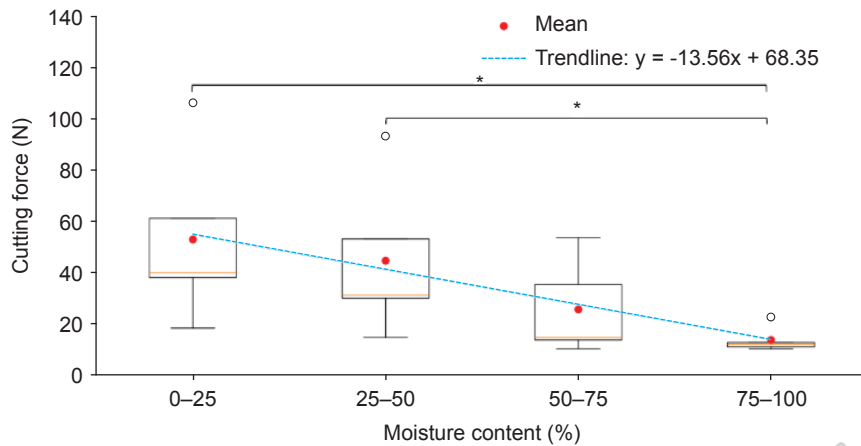


Figure 6. Peak cutting force of oil palm frond (OPF) at different moisture levels. The cutting force becomes lower when the moisture increases. There is a significant difference between groups ( $p < 0.05$ ).

making them more resistant to cutting. As MC decreases, the fronds lose flexibility, leading to greater resistance and higher cutting forces. This behaviour can be explained by the viscoelastic nature of plant tissues. Viscoelasticity refers to materials that exhibit both elastic (spring-like) and viscous (fluid-like) responses to stress. In plant tissues, this property arises from the complex structure of cell walls and the presence of polymers like lignin, which contribute to time-dependent deformation and recovery under load. Water acts as a plasticiser in plant tissues, making cell walls more flexible and easier to deform. When water content drops, the cell walls become more rigid, leading to increased fracture energy and resistance during mechanical processes like cutting (Chaudhuri et al., 2020; Schwaighofer et al., 2023). Another study also reported that the power required increases when the wood MC decreases (dried wood) (Beljo-Lucic et al., 2004). Preethi et al. (2021) investigated the effects of stem diameter, MC and cutting speed on the required cutting force. The results of the required cutting force in the study were similar to the observations made on OPF by Azadbakht et al. (2014). This aligns with the inverse relationship between MC and cutting resistance observed in my study of OPF, where increased MC reduces cutting force, as the material becomes more flexible. However, some study contradicts this concept. A study on tannia cornels demonstrated that the relationship between the cutting force, energy and MC is non-linear, indicating complex interactions between moisture levels and material properties during cutting (Oyefeso et al., 2021).

The SCF and the time taken to cut the fronds were analysed for different moisture levels (Figure 7). For the driest fronds (0%–25% moisture), the SCF is the highest at  $0.07 \pm 0.05$  N, with an average cutting time of  $50.50 \pm 17.80$  s. As MC increased to the 25%–50% range,

the SCF decreased to  $0.03 \pm 0.02$  N, with a cutting time of  $17.60 \pm 6.50$  s. For 50%–75% moisture, the SCF further decreased to  $0.01 \pm 0.01$  N, and the cutting time decreased to  $13.60 \pm 2.30$  s. The highest moisture level (75%–100%) has the lowest SCF of  $0.007 \pm 0.003$  N, with the shortest cutting time of  $19.00 \pm 3.39$  s. The cutting force, SCF and cutting time are affected by MC. The driest fronds exhibited the highest SCF ( $0.07 \pm 0.05$  N) and the longest cutting time ( $50.50 \pm 17.80$  s), whereas the most hydrated fronds had the lowest SCF ( $0.007 \pm 0.003$  N) and shorter cutting times ( $19.00 \pm 3.39$  s). The clear decrease in both SCF and time with increasing moisture suggests that higher water content softens the fronds, making them easier to cut. Hydrated plant tissues are mechanically distinct from their dry counterparts. When tissues are well-hydrated, they have a lower modulus (are less stiff) and greater plasticity, which means they require less energy to cut or deform. This is due to the way water interacts with the polymers and structures within plant cells (Edelmann et al., 2005), reducing the energy needed to initiate and propagate a cut. This highlights how moisture influences the stress-strain behaviour of biological materials during mechanical interaction.

Flexural load results further support these observations. Flexural load tests show an increase with decreasing MC (Figure 8). For fronds at 0%–25% moisture, the mean flexural load is the highest at  $242.38 \pm 59.53$  N. This increased to  $210.86 \pm 61.76$  N for the 25%–50% moisture range, and  $151.03 \pm 24.53$  N for the 50%–75% moisture range. The lowest mean flexural load is observed for fronds at 75%–100% moisture, with a value of  $129.46 \pm 88.64$  N. This increase in flexural load reflects the increased stiffness of the fronds as MC decreases. As MC decreased, the flexural loads increased, with the driest fronds (0%–25% moisture) requiring the highest load of  $242.38 \pm 59.53$  N. This trend reflects the increased stiffness of drier fronds, which aligns

with the Young's modulus results. As tissues dry, lignocellulosic bonding becomes more dominant in determining mechanical stiffness, increasing the resistance to both bending and cutting (Schwaighofer et al., 2023). These findings are important in understanding material failure modes and in designing effective mechanical harvesting systems. The Young's modulus increased from  $229.29 \pm 132.61$  MPa at the highest moisture level to  $1,147.22 \pm 340.88$  MPa at the lowest, confirming that drier fronds are stiffer and less flexible.

Young's modulus, a measure of stiffness, is also found to increase with decreasing MC (Figure 9). For fronds with 0%–25% moisture, the Young's Modulus is the highest at  $1,147.22 \pm 340.88$  MPa. This increased from  $468.20 \pm 83.70$  MPa at 25%–50% moisture,  $329.59 \pm 86.96$  MPa at 50%–75% moisture and  $229.29 \pm 132.61$  MPa at 75%–100% moisture. These values confirm that drier fronds are significantly stiffer.

Porosity measurements show a decrease as MC decreased (Figure 10). The fronds at 0%–25% moisture have the lowest porosity at  $7.33 \pm 1.95\%$ . This increased to  $10.32 \pm 4.11\%$  at 25%–50% moisture,  $12.54 \pm 3.23\%$  at 50%–75% moisture,

and  $36.05 \pm 7.75\%$  at 75%–100% moisture. This trend indicates that the structure of the fronds becomes more compact as moisture is lost. Porosity measurements, on the other hand, show an opposite trend. As MC decreased, porosity also decreased. The fronds with 75%–100% moisture have the highest porosity at  $36.05 \pm 7.75\%$ , while the driest fronds had the lowest porosity at  $7.33 \pm 1.95\%$ . This indicates that when the fronds are losing moisture, their internal structure becomes more compact, likely contributing to their increased stiffness and resistance to cutting.

The reduced porosity observed in drier fronds can be related to lignocellulosic matrix compaction, where dehydration causes closer packing of cellulose, hemicellulose and lignin components, resulting in increased stiffness and reduced voids. Similar microstructural compaction has been reported in other fibrous residues such as sugarcane bagasse (Ouedraogo et al., 2023) and onion bulbs (Huang et al., 2018), which show comparable increases in mechanical rigidity when moisture decreases. This supports the SEM evidence of a denser microstructure in drier OPF samples.

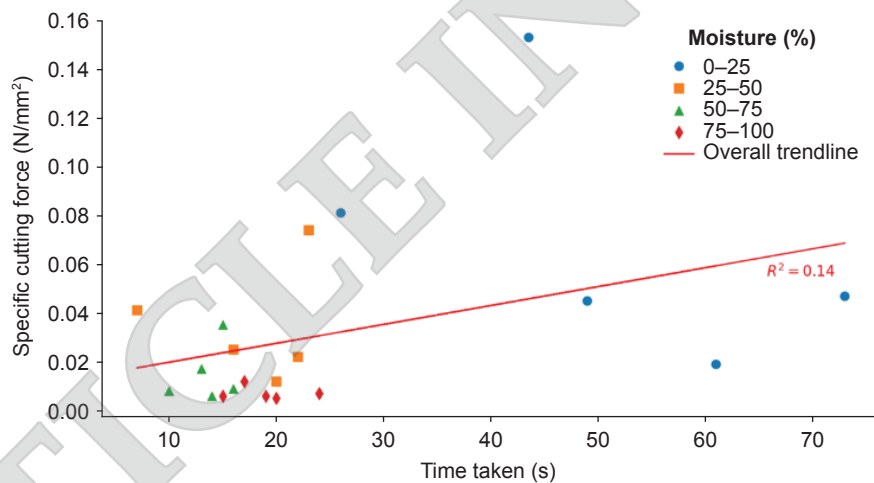


Figure 7. Specific cutting force vs. time taken, with the overall correlation  $R^2 = 0.14$ .

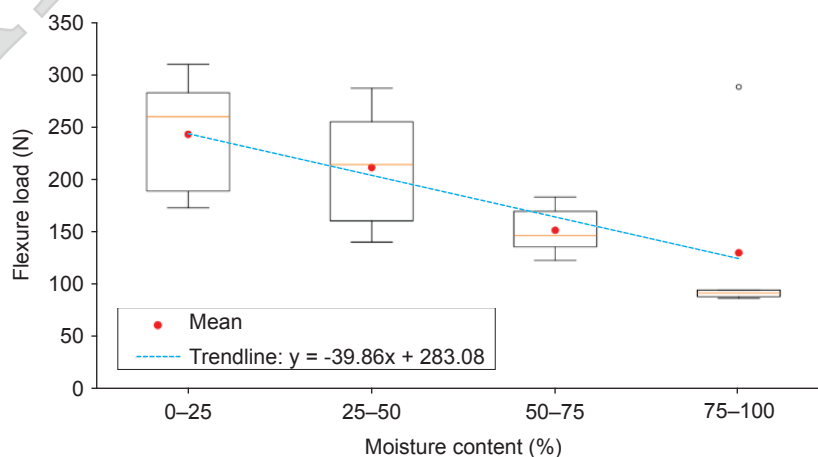


Figure 8. Maximum flexural load of frond over moisture content. Flexure load becomes lower when moisture increases.

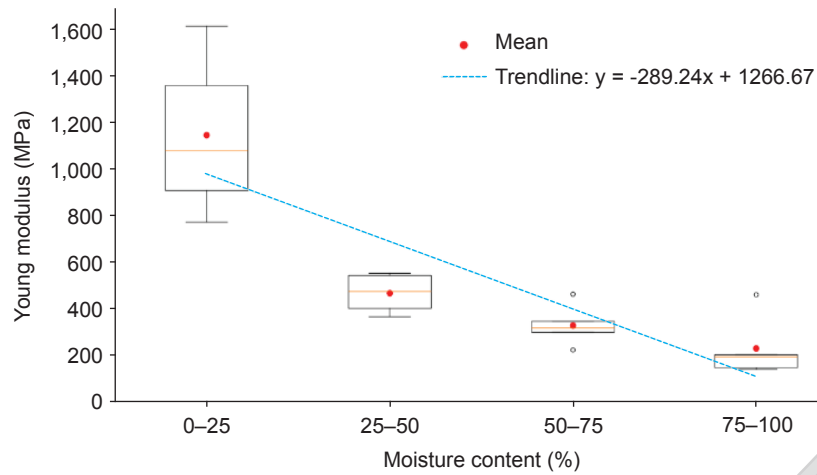


Figure 9. Young's modulus with frond moisture content. Young's modulus significantly decreases with increasing moisture levels.

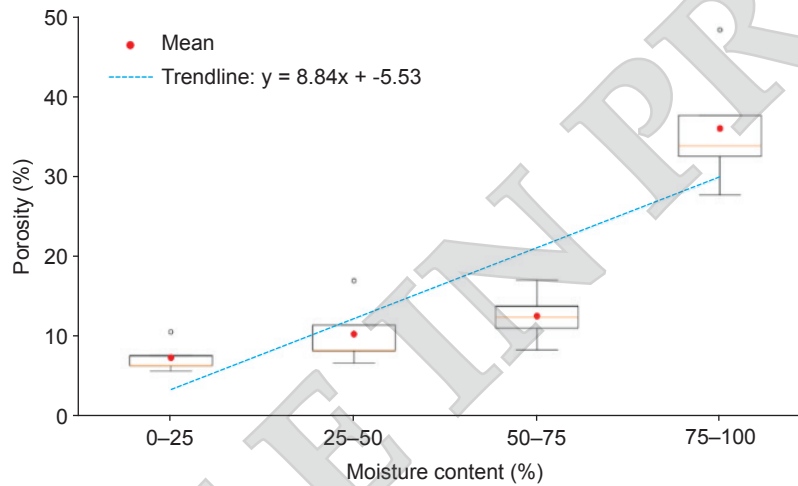


Figure 10. Frond porosity across different moisture content. Porosity increases noticeably as moisture content rises.

Table 2 summarises the mechanical properties of the OPF at different moisture levels, showing that a higher MC leads to a lower cutting force and stiffness, but a higher porosity.

Pearson's correlation analysis reveals significant relationships between the MC and the mechanical properties of the oil palm fronds (Table 3). A negative correlation exists between MC and peak resultant cutting force (Pearson's  $r = -0.5667$ ,  $p = 0.0091$ ), maximum flexural load (Pearson's  $r = -0.6173$ ,  $p = 0.0037$ ) and Young's modulus (Pearson's  $r = -0.8127$ ,  $p = 0.00001$ ), indicating that as MC decreases, the cutting force required increases and the fronds become stiffer and more resistant. Conversely, MC is positively correlated with porosity (Pearson's  $r = 0.8115$ ,  $p = 0.00001$ ), meaning that higher MC results in greater porosity. These correlations underscore the significant influence of MC on cutting force, flexural load, stiffness and porosity in OPF.

These findings, when combined with the broader potential for utilising OPF, highlight

the importance of efficient harvesting methods. According to Ooi et al. (2017), OPF can be repurposed into a variety of products, from biodegradable bio-composites to renewable energy sources and materials for the pulp and paper industry. As such, understanding the mechanical behaviour of the fronds at different moisture levels is not only crucial for optimising harvesting techniques but also for enhancing the economic value of these agricultural by-products.

Understanding the cutting force required for OPF harvesting is fundamental for designing efficient cutting tools with optimised blade geometry and machine power specifications. This study demonstrates that variations in the MC significantly influence cutting resistance, providing requirement input for designing blade design and motor power to real harvesting conditions. Lower cutting forces reduce energy consumption, enhance operator safety by minimising excessive tool vibration and lower the risk of Work-Related Musculoskeletal Disorders (WMSDs) by reducing

TABLE 2. SUMMARY OF THE EXPERIMENTAL RESULTS

Moisture content (%)	Average (mean $\pm$ SD)				
	Peak cutting force (N)	Specific cutting force (N/mm <sup>2</sup> )	Max flexural load (N)	Young's modulus (MPa)	Porosity (%)
0–25	53.00 $\pm$ 2.62	0.070 $\pm$ 0.050	242.38 $\pm$ 59.53	1147.22 $\pm$ 340.88	7.33 $\pm$ 1.95
25–50	44.77 $\pm$ 4.37	0.030 $\pm$ 0.020	210.86 $\pm$ 61.76	468.20 $\pm$ 83.70	10.32 $\pm$ 4.11
50–75	25.92 $\pm$ 2.18	0.010 $\pm$ 0.010	151.03 $\pm$ 24.53	329.59 $\pm$ 86.96	12.54 $\pm$ 3.23
75–100	14.07 $\pm$ 0.68	0.007 $\pm$ 0.003	129.46 $\pm$ 88.64	229.29 $\pm$ 132.61	36.05 $\pm$ 7.75

TABLE 3. PEARSON'S CORRELATION ANALYSIS

Variable		Peak resultant cutting force (N)	Maximum flexural load (N)	Young's modulus (MPa)	Porosity (%)	Moisture content (%)
Peak resultant cutting force (N)	<i>p</i> -value:	-	-	-	-	-
	Pearson's <i>r</i> :	-	-	-	-	-
Maximum flexural load (N)	<i>p</i> -value:	0.2343	-	-	-	-
	Pearson's <i>r</i> :	0.2786	-	-	-	-
Young's modulus (Mpa)	<i>p</i> -value:	0.1273	0.0002	-	-	-
	Pearson's <i>r</i> :	0.3526	0.7444	-	-	-
Porosity (%)	<i>p</i> -value:	0.0345	0.0323	0.0145	-	-
	Pearson's <i>r</i> :	-0.4745	-0.4797	-0.5374	-	-
Moisture content (%)	<i>p</i> -value:	0.0091	0.0037	0.00001	0.00001	-
	Pearson's <i>r</i> :	-0.5667	-0.6173	-0.8127	0.8115	-

physical strain during manual or semi-mechanised operations (Abdullah et al., 2023; Ganesh et al., 2024; Noor & Ridzwan, 2024).

These findings also create prospects for the future development of mechanised oil palm harvesting tools. By understanding the relationship between frond stiffness, moisture and cutting resistance, product designers can further optimise blade geometry, cutting speed and motor efficiency to enhance ergonomics, extend tool lifespan and promote safer, more sustainable harvesting operations.

### Strengths and Limitations of the Study

This study presents a novel experimental approach by combining cutting force analysis with porosity and bending strength measurements on the same frond samples. The use of a controlled lab setup with calibrated sensors ensures consistency and reliability in capturing mechanical behaviour across different MC levels.

However, the findings are limited by the small sample size per group and the use of only one blade type and cutting speed. The absence of field testing also restricts the generalisability of the results. Future studies should explore various blade geometries, operational speeds and real harvesting conditions to strengthen applicability and tool design recommendations.

### CONCLUSION

This study shows that the understanding on the MC is critical for optimising OPF harvesting processes. As MC decreases, the SCF increases, with SCF rising from  $0.007 \pm 0.003$  N at 100%–75% moisture to  $0.07 \pm 0.05$  N at 25%–0% moisture. The results show that the drier fronds show greater cutting force, stiffness and flexural load, while higher moisture levels lead to reduced cutting resistance. By showing these relationships, this research can contribute to the development of more efficient harvesting techniques that enhance productivity and reduce physical strain. Furthermore, the findings also open the door to using OPF in producing value-added products, such as bio-composites, which have potential applications across various industries. Overall, this study provides significant insights into improving agricultural practices while promoting environmentally friendly innovations for OPF consumption.

### ACKNOWLEDGEMENT

The author would like special thanks to Universiti Sains Malaysia for the financial assistance through Bridging Grant (R501-LR-RND003-000000557-0000).

## REFERENCES

- Abdullah, C. K., Jawaid, M., Abdul Khalil, H. P. S., Zaidon, A., & Hadiyane, A. (2012). Oil palm trunk polymer composite: Morphology, water absorption, and thickness swelling behaviours. *BioResources*, 7(3), 2948–2959. <https://doi.org/10.15376/biores.7.3.2948-2959>
- Abdullah, N. A., Mohamad Shaberi, M. N., Nordin, M. N. A., Mohd Ripin, Z., Razali, M. F., Wan Mamat Ali, W. M. A., Awang, B., & Ridzwan, M. I. Z. (2023). Field measurement of hand forces of palm oil harvesters and evaluating the risk of work-related musculoskeletal disorders (WMSDs) through biomechanical analysis. *International Journal of Industrial Ergonomics*, 96, 103468. <https://doi.org/10.1016/j.ergon.2023.103468>
- Ahmad, M. (2024). Evaluation and comparison of the ergonomics, performance and economics of battery-powered and engine-powered palm oil harvesting tools: Cantas elektro. *Jurnal Kejuruteraan*, 35(4), 811–821. [https://doi.org/10.17576/jkukm-2023-35\(4\)-03](https://doi.org/10.17576/jkukm-2023-35(4)-03)
- Azadbakht, M., Asl, A. R., & Zahedi, K. (2014). Energy requirement for cutting corn stalks (Single Cross 704 Var.). *Zenodo* (Single Cross 704 Var). World Academy of Science, Engineering and Technology. *International Journal of Biological, Biomolecular Agricultural, Food and Biotechnological Engineering*, 8, 479–482.
- Beljo-Lucic, R., Goglia, V., Dukic, I., & Risovic, S. (2004). The influence of wood moisture content on the process of circular rip-sawing. Part I: Power requirements and specific cutting forces. *Wood Research*, 49(1), 41–49.
- Chan, Y. S., Teo, Y. X., Gouwanda, D., Nurzaman, S., Gopalai, A., & Thannirmalai, S. (2022). Musculoskeletal modelling and simulation of oil palm fresh fruit bunch harvesting. *Scientific Reports*, 12, 8010. <https://doi.org/10.1038/s41598-022-12088-6>
- Chaudhuri, O., Cooper-White, J., Janmey, P. A., Mooney, D. J., & Shenoy, V. B. (2020). Effects of extracellular matrix viscoelasticity on cellular behaviour. *Nature*, 584, 535–546. <https://doi.org/10.1038/s41586-020-2612-2>
- Edelmann, H., Neinhuis, C., & Bargel, H. (2005). Influence of hydration and temperature on the rheological properties of plant cuticles and their impact on plant organ integrity. *Journal of Plant Growth Regulation*, 24, 116–126. <https://doi.org/10.1007/s00344-004-0015-5>
- Ganesh, U., Ripin, Z. M., Ali, W. M. A. W. M., Heng, Y. Y., Law, M. J. J., Karunakaran, J., & Ridzwan, M. I. Z. (2024). A biomechanical analysis on work-related musculoskeletal disorders using a mechanised chainsaw for oil palm harvesting. *Journal of Oil Palm Research*, 37(4), 684–695. <https://doi.org/10.21894/jopr.2024.0045>
- Ganesh, U., Ripin, Z. M., Ali, W. M. A. W. M., & Ridzwan, M. I. Z. (2025). Effects of saw blade geometry on oil palm frond cutting. *Jordan Journal of Mechanical and Industrial Engineering* 19(3), 657–668. <https://doi.org/10.59038/jjmie/190317>
- Guangul, F. M., Sulaiman, S. A., Moni, M. N., At Naw, S. M., & Konda, R. E. (2013). Determination of the equilibrium moisture content of oil palm fronds feedstock for gasification process. *Asian Journal of Scientific Research*, 6(2), 360–366. <https://doi.org/10.3923/ajsr.2013.360.366>
- Hamdan, M., Sabudin, S., Faizal, M., & Raghavan, V. R. (2012). Experimental studies on oil palm frond drying using swirling fluidized bed dryer. *AIP Conference Proceedings*, 1440, 1212–1219. <https://doi.org/10.1063/1.4704339>
- Huang, S., Makarem, M., Kiemle, S. N., Zheng, Y., He, X., Ye, D., Gomez, E. W., Gomez, E. D., Cosgrove, D. J., & Kim, S. H. (2018). Dehydration-induced physical strains of cellulose microfibrils in plant cell walls. *Carbohydrate Polymers*, 197, 337–348. <https://doi.org/10.1016/j.carbpol.2018.05.091>
- Noor, U. M., & Ridzwan, M. I. Z. (2024). Prevalence of work-related musculoskeletal disorders (WMSDs) and recent initiatives to address them in the oil palm industry: A systematic review. *Journal of Oil Palm Research*, 37(4), 581–597. <https://doi.org/10.21894/jopr.2024.0048>
- Moya-Ignacio, M., Sánchez, D., Romero, J. Á., & Villar-García, J. R. (2024). Study of various mechanical properties of maize (*Zea mays*) as influenced by moisture content. *Agronomy*, 14(8), 1613. <https://doi.org/10.3390/agronomy14081613>
- Ooi, Z. X., Teoh, Y. P., Kunasundari, B., & Shuit, S. H. (2017). Oil palm frond as a sustainable and promising biomass source in Malaysia: A review. *Environmental Progress and Sustainable Energy*, 36(6), 1864–1874. <https://doi.org/10.1002/ep.12642>

- Ouedraogo, M., Bamogo, H., Sanou, I., Mazars, V., Aubert, J., & Millogo, Y. (2023). Microstructural, physical and mechanical characteristics of adobes reinforced with sugarcane bagasse. *Buildings*, 13(1), 117. <https://doi.org/10.3390/buildings13010117>
- Oyefeso, B. O., Akintola, A., Afolabi, M. G., Ogunlade, C. A., Fadele, O. K., & Odeniyi, O. M. (2021). Influence of the moisture content and speed on the cutting force and energy of tannia cormels. *Research in Agricultural Engineering*, 67(3), 123–130. <https://doi.org/10.17221/79/2020-rae>
- Ozigi, P. B., Jimoh, A. A., Rahmon, R. O., & Babatunde, O. Y. (2018). Investigation on some physical and mechanical properties of Apa (*Azelia bipindensis*) timber grown in Kwara State, Nigeria. *Journal of Research Information in Civil Engineering*, 15(1), 2028–2044.
- Preethi, R., Saravanakumar, M., Kamaraj, P., & Vallal Kannan, S. (2021). Effect of stem diameter, moisture content and cutting speed on cutting force for groundnut harvesting. *Madras Agricultural Journal*, 108(7–8), 365–369. <https://doi.org/10.29321/maj.10.000531>
- Ratanawilai, T., Chumthong, T., & Kirdkong, S. (2006). An investigation on the mechanical properties of trunks of palm oil trees for the furniture industry. *Journal of Oil Palm Research (Special Issue, April)*, 114–121.
- Saminathan, M., Mohamed, W. N. W., Noh, A. M. D., Ibrahim, N. A., Fuat, M. A., Ramiah, S. K., Chung, E. L. T., & Dian, N. L. H. M. (2022). Treated oil palm frond and its utilisation as an improved feedstuff for ruminants – An overview. *Journal of Oil Palm Research*, 34(4), 591–607. <https://doi.org/10.21894/jopr.2021.0041>
- Schwaighofer, M., Königsberger, M., Zelaya-Lainez, L., Lukacevic, M., Serna-Loaiza, S., Harasek, M., Zikeli, F., Friedl, A., & Füssl, J. (2023). The viscoelastic behavior of lignin: Quantification through nanoindentation relaxation testing on hot-pressed technical lignin samples from various origins. *Mechanics of Materials*, 188, 104864. <https://doi.org/10.1016/j.mechmat.2023.104864>
- Sulaiman, S. A., Guangul, F. M., Konda, R. E., Atnaw, S. M., & Moni, M. N. (2016). Estimation of moisture content of oil palm fronds through correlation with density for the process of gasification. *BioResources*, 11(4), 8941–8952.